Eidgenössische Technische Hochschule Zürich
Swiss Federal Institute of Technology Zurich

WASSERBILANZ UND TROCKENHEIT

M. HIRSCHI, E.L. DAVIN, C. SCHWINGSHACKL, R. WARTENBURGER, R. MEIER, L. GUDMUNDSSON UND S.I. SENEVIRATNE

IM AUFTRAG DES BUNDESAMTES FÜR UMWELT BAFU – *November 2019*

EIN FORSCHUNGSPROJEKT IM RAHMEN DES NCCS THEMENSCHWERPUNKTES “HYDROLOGISCHE GRUNDLAGEN ZUM KLIMAWANDEL” DES NATIONAL CENTRE FOR CLIMATE SERVICES

Impressum

Commissioned by: Federal Office for the Environment (FOEN), Hydrology Division, CH-3003 Bern. The FOEN is an agency of the Federal Department of the Environment, Transport, Energy and Communications (DETEC).

Contractor: ETH Zürich, Institute for Atmospheric and Climate Science, Universitätstrasse 16, CH-8092 Zürich

Authors: Martin Hirschi, Edouard L. Davin, Clemens Schwingshackl, Richard Wartenburger, Ronny Meier, Lukas Gudmundsson, Sonia I. Seneviratne

FOEN support: Fabia Huesler, Petra Schmocker-Fackel

Note: This project report was prepared under contract to the Federal Office for the Environment (FOEN). The contractor bears sole responsibility for the content.

Citation: M. Hirschi, E.L. Davin, C. Schwingshackl, R. Wartenburger, R. Meier, L. Gudmundsson, and S.I. Seneviratne, 2019. “Wasserbilanz und Trockenheit”. Hydro-CH2018 project report. Commissioned by the Federal Office for the Environment (FOEN), Bern, Switzerland, 20 pp, doi:10.3929/ethz-b-000393212

DOI: 10.3929/ethz-b-000393212 (https://doi.org/10.3929/ethz-b-000393212)

Zusammenfassung

Das Hydro-CH2018 Forschungsprojekt “Wasserbilanz und Trockenheit” führte eine beobachtungs- und prozessbasierte Evaluation der CH2018 Szenarien durch und untersuchte diese hinsichtlich der prognostizierten Änderungen der Verdunstung, der Bodenfeuchte und verschiedener Wasserbilanzindikatoren für Europa und die Schweiz.

Einerseits wurden beobachtungsbasierte Dürre- und Wasserbilanzindikatoren verwendet, um die CH2018 Szenarien und deren Unsicherheit zu untersuchen. Anderseits wurde die Rolle von Prozessen analysiert, welche in den CH2018 Szenarien nicht berücksichtigt werden. Im Speziellen sind dies a) die Rolle von Bewässerung, b) die Darstellung von pflanzenphysiologischen Effekten in den regionalen Klimamodellen und c) Landnutzungsänderungen. Mit Hilfe von mechanistischen Modellsimulation mit dem regionalen Klimamodell COSMO-CLM$_2$ wurde die Sensitivität der prognostizierten Klimaänderung bezüglich dieser Prozesse quantifiziert. Zusätzlich wurden die CH2018 Szenarien hinsichtlich den Temperaturzielen (2° C gegenüber 1.5° C) des Pariser-Abkommens dargestellt und untersucht.

Für den Sommer und eine starke Erwärmung prognostizieren die CH2018 Szenarien in der Schweiz bis zum Ende des Jahrhunderts eine Reduktion von Regentagen und damit verbunden eine Tendenz für längere Trockenperioden. Die mit der Erwärmung verbundene zusätzliche Verdunstung führt dabei zu einer verstärkten Austrocknung der Böden. Dementsprechend zeigen die untersuchten Dürre- und Wasserbilanzindikatoren bezüglich der globalen Mitteltemperatur für den Alpenraum eine Tendenz zu verstärkter Trockenheit. Im Gegensatz zu Temperaturextremen zeigen sich für diese Indikatoren jedoch keine signifikanten Unterschiede zwischen dem 2° und 1.5° C globalen Temperaturziel.

Der Umfang der Zunahme der Sommertrockenheit in der Schweiz ist mit grösseren Unsicherheiten behaftet, da die Schweiz in einer Übergangszone zwischen Südeuropa, wo eine starke Zunahme des Dürrerisikos prognostiziert wird, und Nordeuropa, wo mit feuchteren Wintern gerechnet wird, liegt. Die Evaluation der CH2018 Szenarien zeigt, dass die simulierten Dürre- und Wasserbilanzindikatoren im Mittel relativ gut mit den beobachtungsbasierten Indikatoren übereinstimmen. Hingegen trägt die Repräsentation von Prozessen in den regionalen Klimamodellen zur Unsicherheit in den CH2018 Szenarien bei. Namentlich die Berücksichtigung des im Projekt untersuchten pflanzenphysiologische CO_2 Effekts in COSMO-CLM$_2$ führt zu einer Reduktion der Verdunstung in Zentral- und Nordeuropa und damit verbunden zu einer Rückkopplung auf die zukünftige Entwicklung der Temperatur und signifikant höheren Temperaturextremen. Die prognostizierte jährliche maximale Tagestemperatur steigt dadurch etwa um zusätzliche 0.6° C (0.1° C in Südeuropa, 1.2° C in Nordeuropa) bis Ende des Jahrhunderts.

Der vom Klimawandel getriebene Bewässerungsbedarf für die Schweiz verdoppelt sich gemäss COSMO-CLM$_2$ bis Ende des Jahrhunderts. Dieses Signal wird vor allem durch das Tessin, das untere Wallis und die Region Basel dominiert. Die daraus resultierenden Rückkopplungen auf den Wasserkreislauf und die untersuchten Dürre- und Wasserbilanzindikatoren sind jedoch klein und primär in Südeuropa sichtbar. Desweitern zeigen die Simulationen mit dem CLM Landoberflächenmodell grosse Unsicherheiten bezüglich des Effekts von Landnutzungsänderungen auf die Verdunstung in der Schweiz, was eine Aussage zu zukünftigen Auswirkungen nicht zulässt.

Résumé

Sur la base des scenarios climatiques CH2018, le projet Hydro-CH2018 «bilan hydrique et sècheresses» s'est attaché à étudier, pour l'Europe et la Suisse, les changements récents et futurs d'évapotranspiration, d'humidité du sol et de différents indicateurs hydrologiques.

D'une part, des données observationnelles ont été utilisées pour évaluer les simulations climatiques CH2018 et quantifier leurs incertitudes du point de vue hydrologique. D'autre part, le rôle de processus non pris en compte dans les scenarios climatiques CH2018 a été examiné. Il s'agit plus particulièrement a) de l'irrigation, b) de l'effet physiologique du CO_2 sur les plantes et c) des changements d'usage des terres. Avec l'aide du modèle climatique régional COSMO-CLM$_2$, la sensibilité des projections climatiques a la représentation de ces processus a été quantifiée. De plus, les scenarios climatiques CH2018 ont été analysés sous l'angle de l'accord de Paris sur le climat (objectif de contenir le réchauffement global sous 2° C et si possible 1.5° C).

Les scenarios climatiques CH2018 projettent d'ici la fin du siècle, pour la Suisse et pour un scenario de forte augmentation des émissions, une réduction du nombre de jours pluvieux en été associée à une tendance à l'allongement des périodes sèches. L'augmentation de l'évapotranspiration liée à la hausse de température conduit à un assèchement plus fort des sols. En conséquence, la tendance à l'augmentation des sècheresses dans l'arc alpin est proportionnelle à la hausse de la température globale. Cependant, et contrairement aux températures extrêmes, les différents indicateurs de sècheresses ne montrent pas de différences significatives entre 2° et 1.5° C de réchauffement global.

L'ampleur de l'augmentation des sècheresses estivales est très incertaine pour la Suisse du fait de sa situation dans une zone de transition entre l'Europe du Sud, où une forte augmentation des sècheresses est attendue, et l'Europe du Nord, où à l'inverse des hivers plus humides sont pronostiqués. L'évaluation des simulations CH2018 indique que celles-ci sont en général en accord avec les données observées pour différents indicateurs hydrologiques et de sècheresse. Une autre source d'incertitude est liée à des processus absents des scenarios climatiques CH2018. Notamment, la prise en compte de l'effet physiologique du CO_2 sur les plantes dans COSMO-CLM$_2$ indique une diminution de l'évapotranspiration en Europe Centrale et du Nord qui entraine, par rétroaction, une augmentation plus forte des températures extrêmes. Les températures maximales annuelles augmentent ainsi de 0.6° C (0.1° C en Europe du Sud, 1.2° C en Europe du Nord) d'ici la fin du siècle par rapport aux simulations ne prenant pas en compte cet effet physiologique.

D'après les simulations du modèle COSMO-CLM$_2$, les besoins en irrigation en Suisse sont amenés à doubler d'ici la fin du siècle à cause du changement climatique. Cette tendance est principalement dominée par la partie Sud de la Suisse (Valais et Tessin). En revanche, la prise en compte de l'irrigation dans les scenarios climatiques affecte seulement marginalement le cycle de l'eau et le climat à l'exception de l'Europe du Sud. De plus les simulations avec le modèle de surface CLM révèlent de grosses incertitudes concernant l'effet de l'usage des terres sur l'évapotranspiration, rendant difficile un pronostique fiable de l'impact sur le cycle hydrologique.

1 Project overview

1.1 Main outcomes

- In response to strong warming, Switzerland is expected to experience a reduction in wet days and a tendency toward longer dry spells (meteorological drought) in summer by the end of the century. The associated increase in evaporative demand is further projected to lead to more pronounced agricultural droughts (drier soils).
- The extent of the projected summer drying, however, remains uncertain (both insignificant and very strong changes cannot be excluded). This is also due to the location of Switzerland in between southern Europe that is projected to experience a severe increase in drought risk, and northern Europe that is expected to experience a winter wetting.
- While the applied drought and water balance indices compare reasonably well with observed indices, process representation in the regional climate models used for the scenario assessment contribute to the reported uncertainties in the CH2018 projections.
- Namely the representation of plant-physiological CO_2 effects may contribute to a reduction in evapotranspiration in Central and Northern Europe and consequent feedbacks on (extreme) temperatures.
- Simulated irrigation demand is projected to increase twofold in Switzerland although feedbacks on the hydrological cycle are generally very small and mostly limited to Southern Europe and the Southern part of Switzerland.

1.2 Motivation

The Hydro-CH2018 research project “Wasserbilanz und Trockenheit” on the one hand provided an assessments of changes in evapotranspiration, soil moisture and water-balance drought indicators for Europe and Switzerland based on the CH2018 projections, and on the other hand quantified the role of some of the key processes for these projections, with focus on the water cycle. In particular, the project investigated the role of human water management and the representation of plant-physiology for the projected changes in the water balance, both aspects that are not considered in the regional climate models (RCMs) forming the basis of the CH2018 projections.

“In summer, a reduction in wet days and a tendency toward longer dry spells (meteorological droughts, i.e., periods with no rain) is expected in response to strong warming (RCP8.5 at the end of the 21st century, low to medium confidence). In addition, there will be an increasing evaporative demand, which is projected to lead to more pronounced agricultural droughts (drier soils, medium confidence). In comparison to temperature and precipitation extremes, the extent of the drying remains more uncertain.” (CH2018)

This statement from the Executive Summary of the CH2018 technical report highlights the inherent uncertainties of current drought projections for Switzerland. The extent of the projected summer drying remains uncertain (both insignificant and very strong changes cannot be excluded) and partly depends on the region. This is on one hand related to the fact that Switzerland is located between southern Europe that is projected to experience a severe increase in drought risk, and northern Europe that will receive more winter precipitation. On the other hand, large natural climate variability and model uncertainties in the representation of key processes (e.g., strength of soil moisture-atmosphere feedbacks, circulation changes), as well as factors such as aerosol forcing, plant-physiology, irrigation, and land-use changes contribute to the uncertainty in these projections.

1.3 Research topics

Within the project, the CH2018 scenarios and their uncertainties were assessed

a) by using observation-based drought and water-balance indices to evaluate the CH2018 multi-model projections (Section 3),
b) by looking at the relation of these indices to global warming and policy-relevant temperature targets (e.g., 2° vs 1.5°, Section 4),
c) as well as by performing mechanistic model experiments to evaluate the sensitivity of the projected climate change and the future water cycle to the representation of irrigation and of the CO_2 effect on plant stomatal conductance, both processes that are not considered in the

CH2018 scenarios (Section 5 – 7). Also, land-use change effects on evapotranspiration were addressed using offline simulations with the CLM land surface model.

Selected project results are presented in the following with short summaries at the beginning of each section. An extended description of all project results is available in the Hydro-CH2018 study "Soil moisture and evapotranspiration" (Section 5 therein) and its appendix[1].

2 Methods

2.1 Model data

The CH2018 multi-model ensemble is based on the EURO-CORDEX RCM simulations (Jacob et al., 2014). The simulations cover the European domain and the 1971–2099 time period. Here, we focus on the historical simulations up to 2005, followed by the RCP8.5 scenario. Lateral boundary conditions and sea surface temperatures (SSTs) are provided by a set of global climate models (GCMs) from the CMIP5 ensemble. Within CH2018, the GCM–RCM model chains were quality controlled and models with obvious issues were excluded from the ensemble (details can be found in the CH2018 technical report, cf. Table 4.1 therein). Only the simulation with the higher resolution is used for RCMs for which both the 0.11º and 0.44º resolutions are available. This resulted in 21 GCM–RCM model chains that are considered in the CH2018 multi-model ensemble.

In addition to the CH2018 multi-model ensemble, dedicated experiments with the regional climate model COSMO-CLM_2 (Davin et al., 2011, 2016; Davin and Seneviratne, 2012) are performed in order to explore the role of processes that are not included in the CH2018 models. Namely, none of the CH2018 models include a representation of irrigation and of the CO_2 effect on plant stomatal conductance (referred as to the plant physiological effect in the following). To test the impact of these processes the following experiments were performed:

(1) a reference simulation with the same setup as for the EURO-CORDEX model ensemble used in CH2018;
(2) one simulation accounting for the plant-physiological effect;
(3) one simulation applying irrigation over crop areas (using the present-day distribution of crops equipped for irrigation).

COSMO-CLM_2 couples the Consortium for Small-scale Modeling (COSMO) atmospheric model in Climate Mode (so called COSMO-CLM) to the Community Land Model (CLM). Here, the version 5.0 of COSMO and the version 4.0 of CLM (Oleson et al., 2010) coupled with OASIS3-MCT is used. The reference experiment is performed using the EURO-CORDEX setup as described above over the time period 1949–2099 with a resolution of 0.44°. The global climate model MPI-ESM-LR under RCP8.5 is used as driving GCM.

In CLM4.0, stomatal conductance is based on the Ball-Berry model (Oleson et al., 2010), which allows stomatal conductance to adjust to CO_2 concentrations. In the second experiment, the CO_2 concentration in the Ball-Berry equation is kept constant (at a level of 367 ppm), whereas in COSMO_PHYS the CO_2 concentration used in the Ball-Berry equation increases according to the RCP8.5 scenario.

In the third experiment, irrigation is simulated using a prognostic model in which irrigation amount is calculated for the irrigated part of the total crop area (total crop area remains identical to the reference simulation and is partitioned into a rainfed and irrigated fraction, the irrigation module being applied only to the latter). The amount of water added is calculated such that plant soil moisture stress is eliminated. For this experiment, the three time slices 1981–2010, 2020–2049 and 2070–2099 are available.

In addition to these simulations, offline simulations with two different versions of the CLM land surface model have been performed in order to display land use change effects on evapotranspiration.

[1] available at https://doi.org/10.3929/ethz-b-000389455

2.2 Observation-based indices

For the evaluation of the RCM simulations, various observational datasets are considered (Table 1). The use of multiple datasets (if available) for a given index provides a robust evaluation of the climate models, and allows to gain insight into the reliability of the observations and to set model biases in relation to the observational uncertainty.

Table 1: Overview on the observation-based datasets and what drought and water-balance indices evaluation they are applied (denoted with X).

Dataset	**Description**	**Indices**[2]					
		SPI	***CDD***	***P-E***	***SMA***	***SRA***	***E***
E-OBS	Gridded observations from E-OBS (Haylock et al., 2008)	X	X				
APGD	Alpine Precipitation Grid Dataset (Isotta et al., 2014)	X	X				
MeteoSwiss	Gridded high-resolution data (RhiresD, RhiresM[3]) from MeteoSwiss	X	X				
CCI-SM	Remote sensing data from the ESA CCI soil moisture project[4] (Dorigo et al., 2017)				X		
LandFlux-EVAL	LandFlux-EVAL Evapotranspiration benchmarking product (Mueller et al., 2013)			X[5]			X
GLEAM	Global Land Evaporation Amsterdam Model (GLEAM) estimation of the different components of land evapotranspiration from satellite data (Martens et al., 2017)						X
WECANN	Estimates of surface turbulent fluxes developed using a machine learning approach informed by remotely sensed solar-induced fluorescence (SIF) and other radiative and meteorological variables (Alemohammad et al., 2017)						X
Fluxnet-MTE	Upscaled observations from the global network of eddy covariance towers (FLUXNET) using a model tree ensemble (MTE) approach (Jung et al., 2009)						X
SWBM	Model-based estimates from the Simple Water Balance Model (SWBM, Orth and Seneviratne 2015) driven with observed meteorological forcing			X[9]	X	X	X
E-RUN	Observation-based gridded runoff estimates for Europe (Gudmundsson and Seneviratne, 2016)					X	

[2] See Table 2
[3] See www.meteoswiss.admin.ch/content/dam/meteoswiss/de/service-und-publikationen/produkt/raeumliche-daten-niederschlag/doc/ProdDoc_RhiresD.pdf and www.meteoschweiz.admin.ch/content/dam/meteoswiss/de/Ungebundene-Seiten/Produkte/doc/ProdDoc_RhiresM.pdf
[4] www.esa-soilmoisture-cci.org/
[5] Combined with E-OBS precipitation

2.3 Indices calculation, domain averaging and statistical evaluation

The drought and water balance indices (Table 2) used for the evaluation of the CH2018 multi-model ensemble and the COSMO-CLM2 simulations are calculated at the grid-cell level of the individual models and of the observational datasets. Except for *CDD*, the indices are thereby calculated on monthly time scale and then seasonally averaged. *CDD* is directly derived for the four seasons as a whole.

Table 2: Drought and water-balance indices used within CH2018 or Hydro-CH2018 "Water balance and droughts".

Index	Description	CH2018	Hydro-CH2018	References
CDD	Maximum number of consecutive dry days (*P<1* mm/day)	X	X	Frich et al. (2002); Alexander et al. (2006); Tebaldi et al. (2006)
SPI3	Standardized precipitation index for 3-months accumulated precipitation	X	X	McKee et al. (1993); Lloyd-Hughes and Saunders (2002)
P-E	Precipitation minus evapotranspiration	X	X	Byrne and O'Gorman (2015); Greve and Seneviratne (2015)
SMA	Standardized soil moisture anomalies	X	X	Orlowsky and Seneviratne (2013)
SRA	Standardized runoff anomalies		X	Gudmundsson and Seneviratne (2015, 2016b)
E	Simulated evapotranspiration		X	

These seasonal grid-cell based indices are then area averaged using the five CH2018 Swiss domains (CH2018 technical report, Figure 2.6 therein) and three European regions defined in the Special Report on Extremes (SREX, Seneviratne et al. 2012b). In addition, the scaling of the indices with global mean temperature (Section 4) also considers the European regions from the PRUDENCE project (Christensen and Christensen, 2007).

Historical trends in the seasonal domain-averaged indices (see Section 3) are estimated by a simple linear regression based on the available time periods of the datasets, and significance of the slope estimate is evaluated using a two-sided Wald Test with t-distribution of the test statistic. A significance level of 5% is chosen. For the observation-based estimates, in addition a minimum temporal coverage of 15 years is required to evaluate trend significance. To test for differences in the means of individual model experiments (see Section 5), a Mann-Whitney-U test is applied (5% significance level).

3 Observational evaluation of CH2018 scenarios

The agreement of the CH2018 multi-model ensemble and the COSMO-CLM2 reference simulation (experiment (1) listed above) are compared with observational datasets (Table 1) for the drought and water-balance indices listed in Table 2. The comparisons are performed for the 1980–2017 time period (or shorter, depending on the availability of observational data).

For most of the assessed drought and water-balance indices, the climate models and the observations generally agree on the historical magnitude and trends. Yet, there are several instances where observations show a significant trend, while there is never a majority of models of the CH2018 multi-model ensemble with significant trends. Additionally, for E and P-E there is a clear bias between the climate models and the observations, especially in Switzerland and Southern Europe. The observational datasets often indicate drying trends in Southern Europe. Also, trends in Switzerland go rather towards drying, although the observational trends in Switzerland are not significant. The CH2018 multi-model ensemble on the average shows very small historical trends for Switzerland, while COSMO-CLM2 shows stronger decreases for P-E, SMA, and SRA in this region.

The maximum number of consecutive dry days (*CDD*) of the CH2018 multi-model ensemble agrees very well with the observations (Figure 1). In Switzerland, Northern and Central Europe, *CDD* lies around 10 days during summer, while it reaches about 50-60 days in Southern Europe.

Both the observations and the CH2018 multi-model ensemble do not show significant trends in *CDD* (Figure 1, lower panel). COSMO-CLM$_2$ tends to overestimates *CDD* compared to the observations in Southern Europe, but is within the range of the CH2018 CORDEX models (Figure A8)[6]. Moreover, and in contrast to observations, COSMO-CLM$_2$ already exhibits a significant increase of *CDD* in Central and Southern Europe throughout the investigated time period (which is also projected for the future, see Section 5).

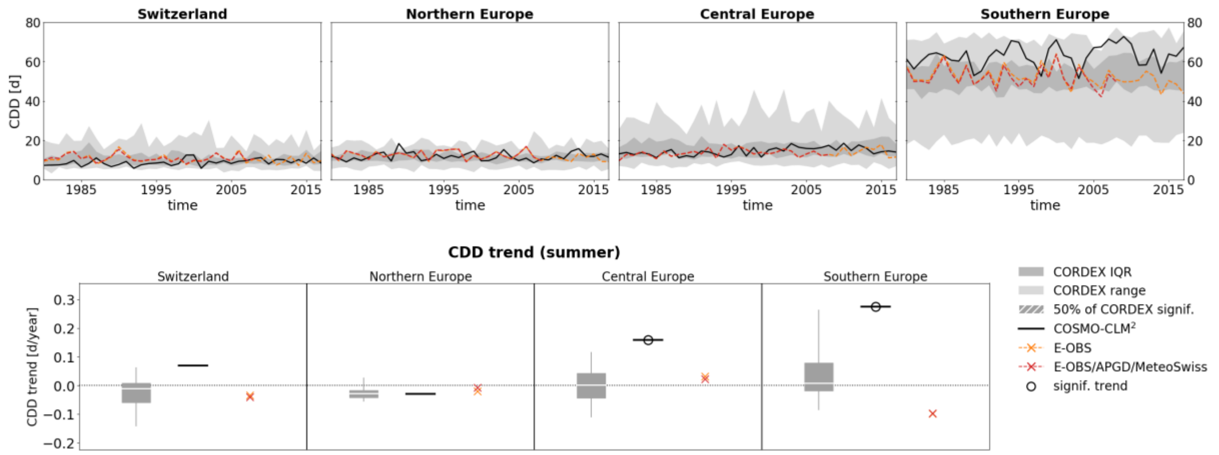

Figure 1: Historical evolution (upper panel) and historical linear trends (lower panel, see Section 2.3) of the maximum number of consecutive dry days (*CDD*) during summer (June, July, August) in Switzerland, Northern Europe, Central Europe, and Southern Europe during 1980–2017. The grey ranges in the upper panel indicate the evolution and spread of the CH2018 CORDEX models, the black line indicates COSMO-CLM$_2$, and the coloured dashed lines indicate the observations. The boxplots in the lower panel indicate the distribution of the CH2018 CORDEX models (white lines indicate the median, boxes the interquartile range and whiskers the 5th and 95th percentiles). Hatching for the CORDEX models indicates 50% of models having a significant trend consistent with the trend in the ensemble median, and circles indicate significant trends for COSMO-CLM$_2$ and the observations (based on a two-sided Wald test with t-distribution of the test statistic, significance level of 5%). For observational datasets it is additionally required that they span a time period of at least 15 years.

The evolution of *SPI3* is shown in Figure 2. By construction there are no (large) biases between the datasets because 1981–2010 is used as reference period for calculating *SPI3* (Figure A9). The CH2018 multi-model ensemble shows a tendency for slightly positive *SPI3* trends in Northern and Central Europe (however mostly not significant at the 5% significance level) and no tendency in Switzerland and Southern Europe. The observations, in contrast, suggest a decrease of *SPI3* in Southern Europe (significant in one of the observational datasets). COSMO-CLM$_2$ also shows a significant negative *SPI3* trend in Southern Europe and as well in Central Europe. The fact that there is no significant *SPI3* trend in Switzerland agrees with the CH2018 report, which found no significant trends in the standardized precipitation evapotranspiration index (SPEI, p.43 CH2018 report).

[6] Here and in the following, Figure A* refers to the Appendix of the Synthesis Report Chapter "Soil moisture and evapotranspiration"

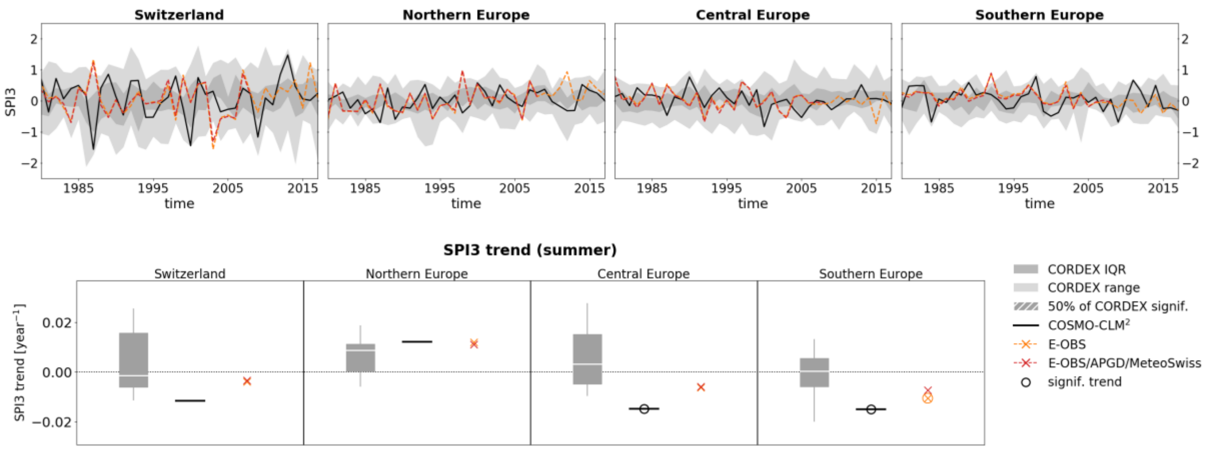

Figure 2: As in Figure 1 but for the 3-month standardized precipitation index (*SPI3*) averaged over summer.

For *P-E*, the climate models often exhibit higher values than the observation-based estimates (Figure 3, upper panel; see also Figure A12). The overestimations are especially pronounced in Switzerland and Southern Europe, suggesting that they are connected to the underestimation of *E* by the climate models. The higher variability in Switzerland is most likely due to the lower number of considered grid cells for the area average. In all regions, the observations exhibit no significant observational trends in *P-E*. The CH2018 multi-model ensemble agrees with this pattern, except for Switzerland where some models tend to exhibit negative trends (mostly not significant). The same also applies for COSMO-CLM$_2$, which has larger negative trends in Switzerland and Central Europe (related to the decrease in summer precipitation in both domains and the increase in *E* in Switzerland).

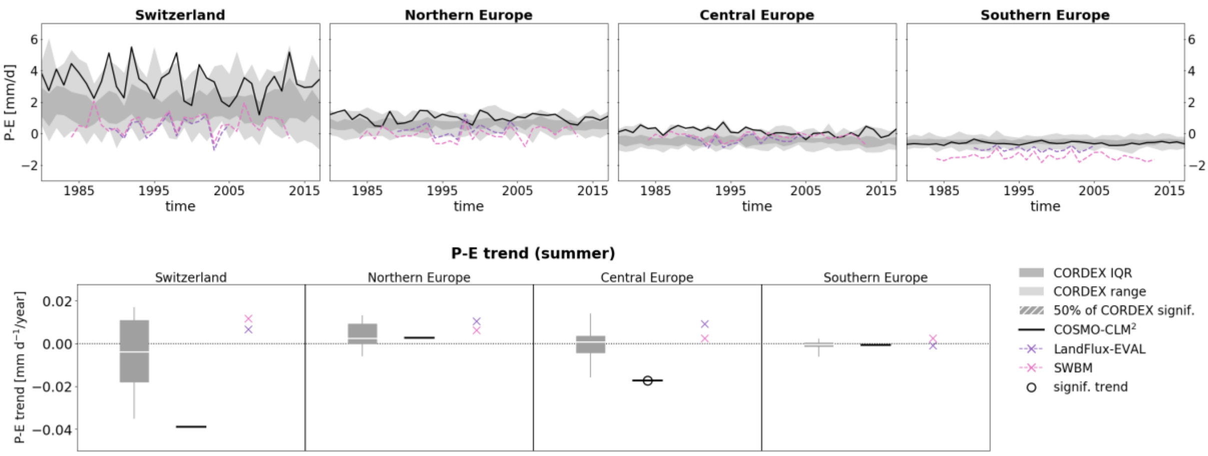

Figure 3: As in Figure 1 but for summer mean of precipitation minus evapotranspiration (*P-E*).

Soil moisture anomalies (*SMA*) in the observations, the CH2018 multi-model ensemble and COSMO-CLM$_2$ are shown in Figure 4. As for *SPI3*, the mean biases are small, as 1981–2010 is used as reference period for calculating *SMA* (Figure A13). The observational datasets show a decreasing *SMA* trend in Northern and Southern Europe, but they do not agree on the sign of the trend in Central Europe and Switzerland. A reason for this might be that CCI-SM only represents surface soil moisture in the top few centimetres of the soil (Dorigo et al., 2017), while SWBM integrates over deeper soil layers (as it calculates soil moisture based on observed precipitation, temperature and net radiation). The CH2018 multi-model ensemble shows a tendency for negative trends in Southern Europe and Switzerland, which are, however, mostly not significant. COSMO-CLM$_2$ also shows significant negative trends in these two regions. The sign of SWBM trend and the median trend of the CH2018 multi-model ensemble generally agree, which hints to the fact that SWBM soil moisture might be better comparable to climate models as it also considers deeper soil layers. Considering Switzerland there is a pronounced disagreement for *SMA* trends in CHS, with CCI-SM exhibiting significant positive and SWBM showing significant negative trends (Figure A6).

The negative SWBM trend in CHS likely reflects the general drying trend in Southern Europe, while the positive CCI-SM trend could reflect increased irrigation (which mostly affects the uppermost soil layers and is not accounted for in SWBM) in Northern Italian grid cells, which are included in the CHS domain and exhibit intensive agriculture and irrigation (see also Figure 12).

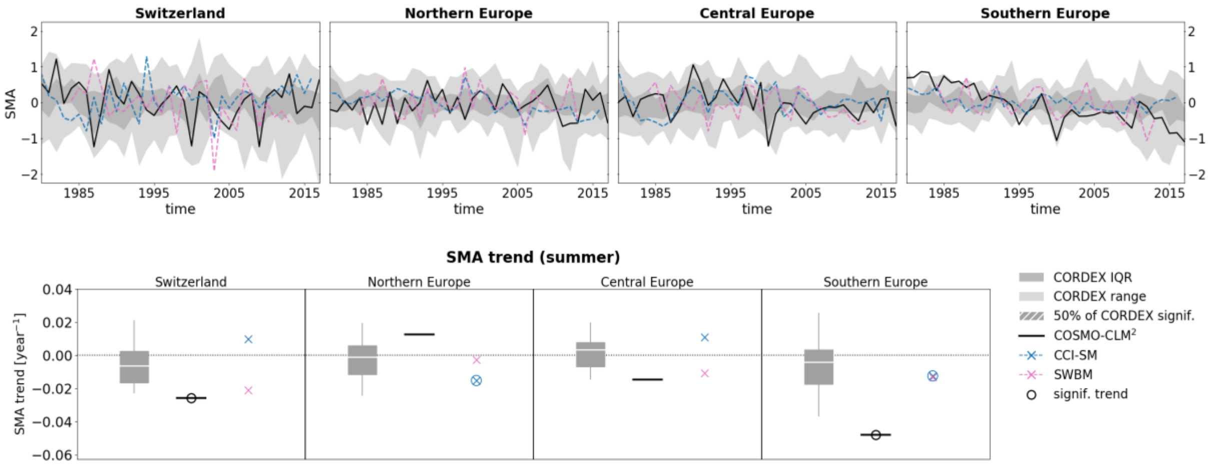

Figure 4: As in Figure 1 but for summer mean soil moisture anomalies (*SMA*).

4 Scaling with global mean temperature

The regional future responses of various climate indices often scale with global mean temperature across emission scenarios and thus with accumulated CO_2 emissions (Seneviratne et al., 2016). These functional relationships between global mean temperature and various climate indices from the CMIP5 model ensemble have been implemented into an interactive plotting framework (Wartenburger et al., 2017)[7] that allows to extract regional climate change impacts based on global temperature targets (such as the 2° C and 1.5° C limits agreed within the 2015 Paris Agreement).

This plotting framework has been expanded within Hydro-CH2018 by the more localized EURO-CORDEX simulations from the CH2018 multi-model ensemble. Results on this smaller regional scale still reveal a quasi-linear scaling of the climate indices with global mean temperature (Figure 5). The analyzed Alpine and CH2018 sub-domains exhibit more pronounced and robust signals towards drying while in the Central European domain, wetting trends in northern part of the domain are mixed with drying trends in the southern part.

The water balance and drought indices reveal clear differences in these functional relationships between Central Europe and the Alpine and CH2018 sub-domains. For *P-E*, all three domains show a drying tendency in summer, which is amplified in the Alpine and the CH2018 domain Northeastern Switzerland (though with larger inter-model spread). For *SMA* and *SRA*, the signals even switch the direction between the domains. The non-existing trend in *SRA* and the positive trend in *SMA* (i.e., wetting) in Central Europe in fact turn into negative trends for both indices for the Alpine and the Swiss domain in summer.

Thus, the Alpine and CH2018 sub-domains exhibit more pronounced and robust signals in the water balance and drought indices while in the Central European domain, wetting trends in northern part of the domain are mixed with drying trends in the southern part, leading to a dilution of the responses. Switzerland, however, is situated at the dry edge of the large-scale European signals (see also CH2018 technical report), which manifests in clearer responses of the water balance and drought indices. The difference between the domains appears most pronounced for *SMA*, i.e., when storage and pre-conditioning effects are considered.

Regarding differences between 2° C and 1.5° C global temperature targets, the water balance and drought indices show only non-significant differences between these two targets both for the larger Central European domain as well as for the smaller Alpine and CH2018 Swiss domains.

[7] http://drought-heat.ethz.ch/atlas/

Lastly, it should be noted that studies indicate differences in climate projections based on RCMs as compared to GCMs (Kjellström et al., 2018; Sørland et al., 2018). The former tend to project a smaller temperature increase than the latter, as well as more precipitation (or less drying). This was hypothesized to be due to discrepant representations of topography, cloud processes, or aerosol forcing in RCMs and GCMs. In addition, the consideration of the plant-physiological CO_2 effect in most GCMs, but generally not in RCMs, may play a key role in explaining this difference (see Section 6). At higher CO_2 concentrations, plants close their stomata openings, which can reduce evapotranspiration and result in feedbacks to temperature. This process may account for 67% of the stronger annual maximum temperature increase in GCMs compared to RCMs.

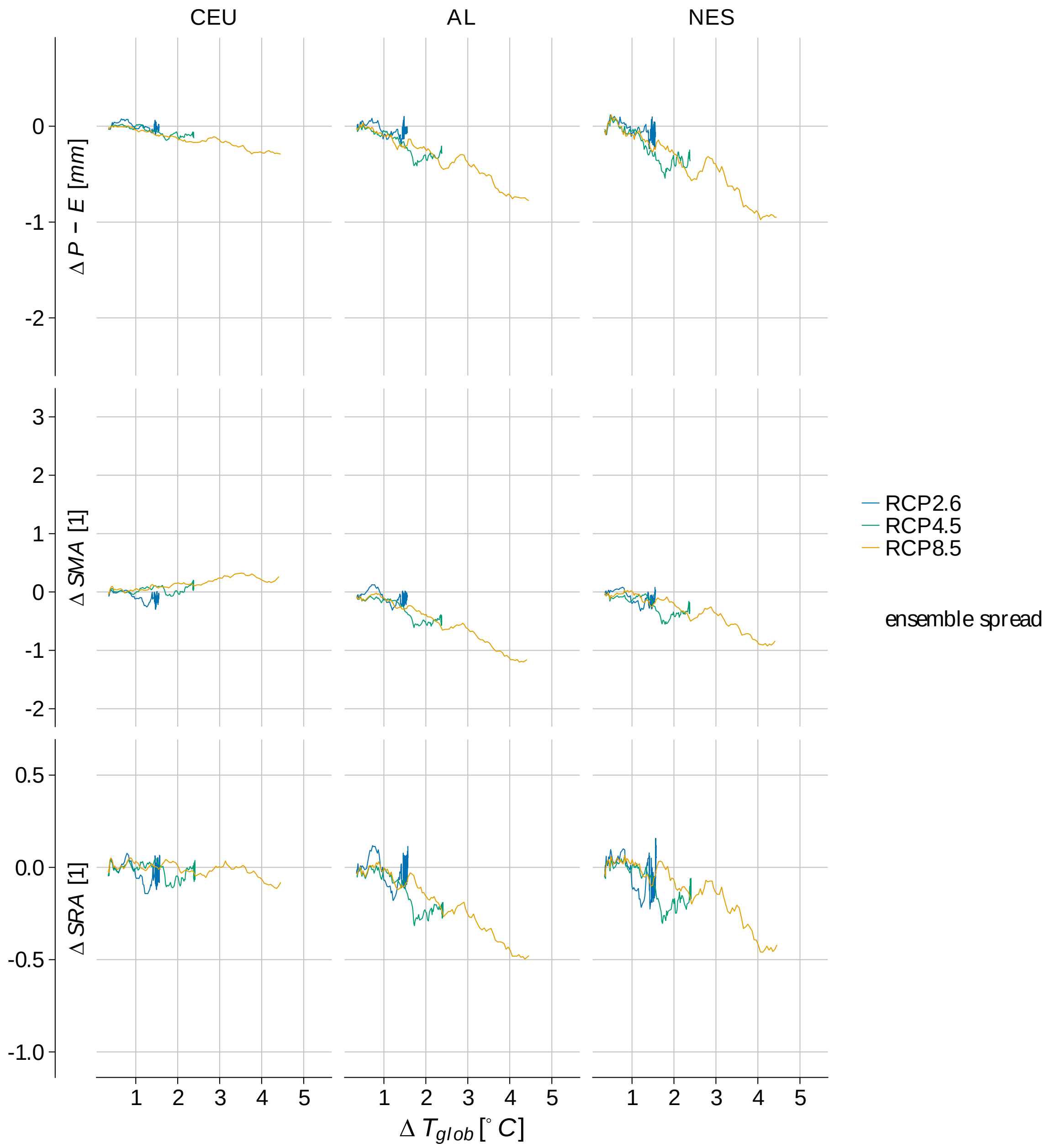

Figure 5: Scaling of the indices *P-E*, *SMA* and *SRA* with global mean temperature in the Central European domain (left column), the larger Alpine region (middle column) and the CH2018 domain Northeastern Switzerland (right column). Summertime changes in the indices are displayed relative to 1971–1990, while the global mean temperature anomaly is adjusted for the warming since the pre-industrial time period (offset of 0.3°C). Plots are based on http://drought-heat.ethz.ch/atlas/.

5 Temporal future changes

Projected temporal future changes in the hydrological cycle during summer (June, July, August) are presented here using the CH2018 multi-model ensemble and two COSMO-CLM$_2$ simulations: the simulation which takes into account plant-physiological CO_2 effects but does not consider irrigation, and the one that additionally considers irrigation (experiments (2) and (3) listed above).

Future projections of changes of the hydrological cycle exhibit a strong drying trend in Southern Europe (reflected in all investigated variables but P-E) and only slight changes in Central and Northern Europe (with Central Europe having a drying tendency and Northern Europe rather a wetting tendency). Due to the geographical location of Switzerland, it combines both features of Southern and European climate change and, additionally, has some remarked changes in the Alpine regions. As a consequence, the projections for Switzerland are often more uncertain (especially for SPI, E, and P-E). The five considered Swiss regions sometimes show diverse trends and local assessments should thus consider the projected evolutions in the single regions.

The CH2018 multi-model ensemble projects that *CDD* will substantially increase in Southern Europe, Central Europe, and Switzerland, but only slightly increase in Northern Europe (Figure 6). By the end of the 21st century, *CDD* will extend by about 2-5 days in Switzerland and Central Europe and by about 5-10 days in Southern Europe. For Switzerland, the most pronounced increase in *CDD* is possible for CHS, however with a large uncertainty (Figure A22).

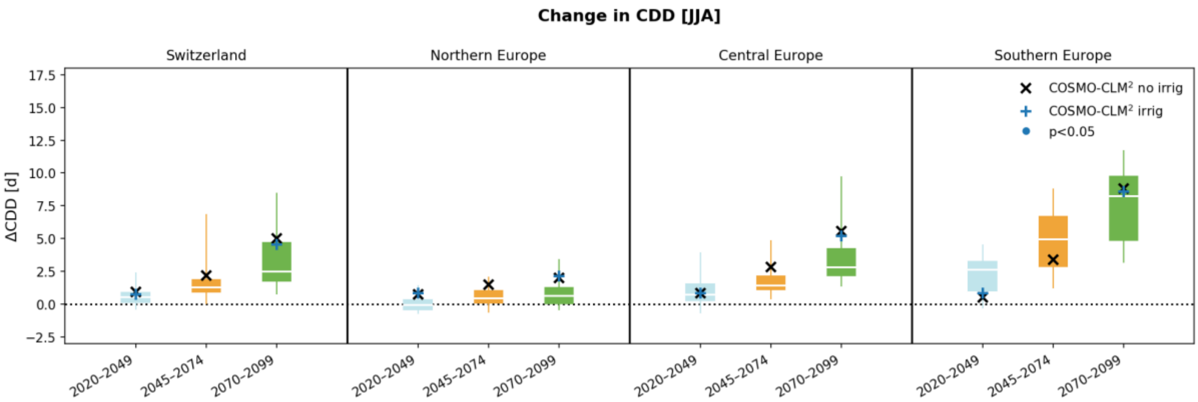

Figure 6: Future changes of the maximum number of consecutive dry days (Δ*CDD*) during summer (June, July, August) in Switzerland, Northern Europe, Central Europe, and Southern Europe during 2020–2049 (light blue boxplots), 2045–2074 (orange boxplots), and 2070–2099 (green boxplots) relative to the 1981–2010 reference period. Black crosses (blue plus signs) indicate the changes in COSMO-CLM$_2$ without (with) irrigation effects. Blue dots indicate whether the COSMO-CLM$_2$ irrigation simulation differs significantly from the one without irrigation (based on a Mann-Whitney-U test with a 5% significance level). Note that for the 2045–2074 time period no data for the COSMO-CLM$_2$ irrigation simulation are available (see Section 2.1) The boxplots indicate the distribution of the CH2018 CORDEX models (white lines indicate the median, boxes the interquartile range and whiskers the 5th and 95th percentiles).

SPI3 is projected to slightly increase in Northern Europe, slightly decrease in Central Europe, and strongly decrease in Southern Europe (Figure 7). Switzerland, which combines the signals of the Mediterranean and Central European climate zones, exhibits a wide range of possible *SPI3* changes, ranging from no change to a strong drying comparable to the reduction in Southern Europe. Strong *SPI3* decreases are mostly projected for the Swiss regions CHW, CHS, and CHAW, albeit with substantial uncertainties (Figure A23).

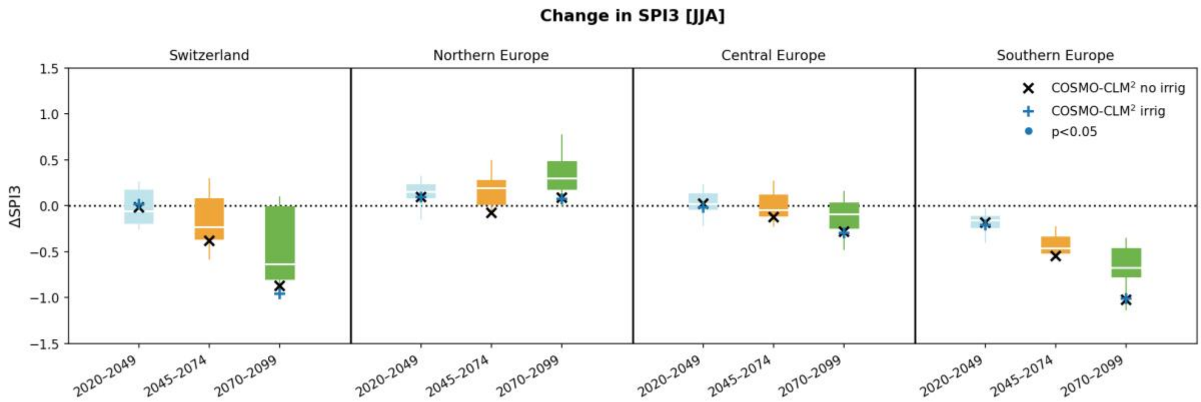

Figure 7: As in Figure 6 but for the 3-month standardized precipitation index (*SPI3*) averaged over summer.

For *P-E*, the CH2018 multi-model ensemble projects a strong decrease in Switzerland and moderate decreases in Northern and Central Europe (Figure 8). In Southern Europe, *P-E* remains almost constant. *P-E* decreases are happening in all Swiss regions, but they are strongest in CHAE and CHAW, suggesting that Alpine climate change substantially affects *P-E*. The strong decrease of *P-E* in Switzerland is both connected to a projected precipitation decrease (Figure 7) and an increase in evapotranspiration.

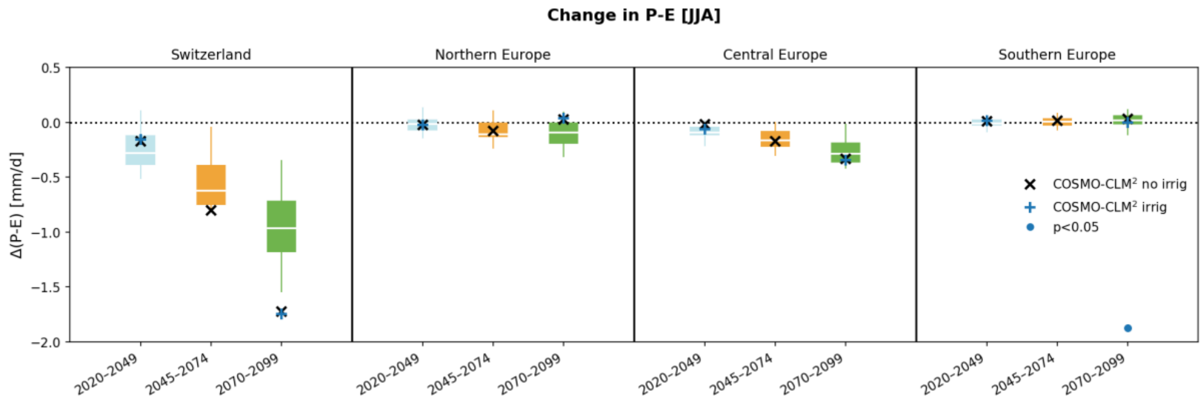

Figure 8: As in Figure 6 but for summer mean of precipitation minus evapotranspiration (*P-E*).

Soil moisture (*SMA*) is projected to decrease in all regions except Central Europe, where trends are only small (Figure 9). Especially in Southern Europe, but also in Switzerland, *SMA* decreases are strong, with some climate models projecting a decrease of 2 to 3 standard deviations. In Switzerland, *SMA* decreases are strongest in the Alpine regions CHAE and CHAW, which appears to be related to carry-over effects due to less snow storage and earlier spring snow melt (see also CH2018 technical report, Chapter 6.7 therein).

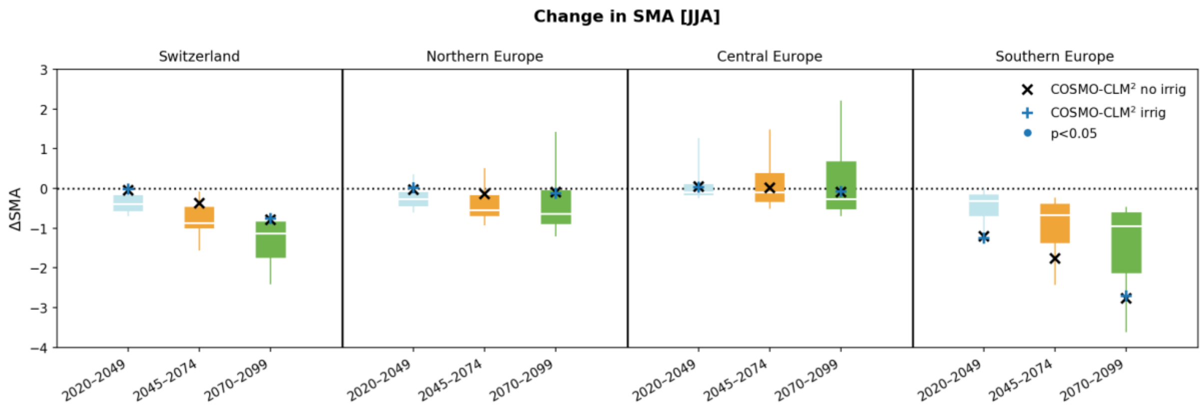

Figure 9: As in Figure 6 but for soil moisture anomalies (*SMA*).

6 Plant-physiological CO_2 effect on evapotranspiration and impact on temperature extremes

(These results have been published in Schwingshackl et al. 2019)
The sensitivity of projected climate change and the future water cycle to the representation of the CO_2 effect on plant stomatal conductance is analyzed using COSMO-CLM$_2$ and compared to the CH2018 multi-model ensemble (which ignores this effect) and various CMIP5 GCM simulations (which mostly consider this effect).

Embedding plant physiological responses to elevated CO_2 concentrations in COSMO-CLM$_2$ leads to pronounced ET decreases in central and northern Europe, but only small ET reductions in southern Europe. The consequent feedback on temperature results in significantly higher projected extreme temperatures in Europe. Annual maximum temperatures rise additionally by about 0.6 K (0.1 K in southern, 1.2 K in northern Europe) by 2070–2099, explaining about 67% of the stronger annual maximum temperature increase in GCMs compared to RCMs. These results highlight the need to include plant physiological CO_2 responses in RCMs in order to provide unbiased regional climate projections that are physically consistent with the driving GCMs.

Most of the GCMs participating in the Coupled Model Intercomparison Project phase 5 (CMIP5) consider plant physiological responses to CO_2 increase (Swann et al., 2016) and show that stomatal adaptation can substantially affect the hydrological cycle (Hong et al., 2018; Lemordant et al., 2018) and even contribute to the amplification of future heat extremes (Lemordant and Gentine, 2019; Skinner et al., 2018). Despite the importance of this process, and in contrast to most GCMs, RCMs generally do not consider plant physiological CO_2 responses. We hypothesize that this systematic discrepancy might be partly responsible for the fact that RCMs predict a smaller temperature increase than GCMs over several European regions (Sørland et al., 2018).

To evaluate differences in future climate projections between GCMs and RCMs, 21 GCM-RCM model chains of EURO-CORDEX are used (see Section 2.1). According to the respective model descriptions, none of the RCMs but seven out of the nine driving GCMs consider plant physiological CO_2 responses. To focus on the question of whether the choice of GCM or RCM simulations changes climate projections over the European domain, we compare the 21 RCM simulations to the simulations of the nine driving GCMs. By only using the driving GCMs we can discriminate any potential effects that would be introduced through an enlargement to the full CMIP5 model ensemble.

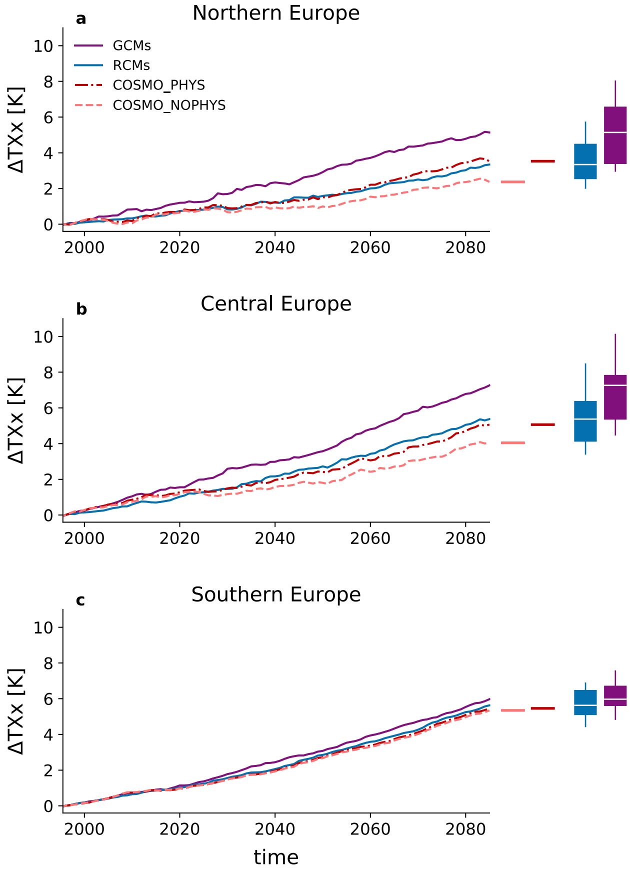

Figure 10: Future projections of annual maximum temperature (TXx). TXx evolution in (a) northern Europe, (b) central Europe, and (c) southern Europe between 1995 and 2085 (30-year moving average) relative to 1981–2010 for RCMs, GCMs, COSMO_PHYS, and COSMO_NOPHYS. Shading for RCMs and GCMs represents the total model range, lines denote the median. The red lines on the right mark the mean ΔTXx during 2070–2099 for COSMO_PHYS and COSMO_NOPHYS, the box-and-whisker-plots indicate the median (line), interquartile range (boxes) and total range (whiskers) of the ΔTXx distribution in GCMs and RCMs during 2070–2099.

The considered GCMs exhibit an amplified future increase of the annual maximum temperature (TXx) compared to the RCMs (violet and blue shadings in Figure 10). The TXx amplification is strongest in central and northern Europe but only small in southern Europe. Additionally, the inter-model spread in both RCMs and GCMs is large in central and northern Europe but narrower in southern Europe. The amplified TXx increase in GCMs in central and northern Europe is consistent with the expectation that plant physiological CO_2 effects on temperature are strongest in regions, which are not water limited (Skinner et al., 2018).

To test the hypothesis that the missing plant physiological CO_2 response in RCMs contributes to the evident GCM-RCM difference, two distinct simulations with a state-of-the-art regional climate model (COSMO-CLM$_2$, see Section 2.1) are performed. The simulations cover the European domain and range from 1970 to 2099, employing the RCP8.5 scenario (Riahi et al., 2011). One COSMO-CLM$_2$ simulation follows the standard EURO-CORDEX setup and does not include plant physiological responses (hereafter denoted as 'COSMO_NOPHYS'), while the second simulation includes plant physiological responses to rising CO_2 concentrations ('COSMO_PHYS', see Section 2.1). Consistent with the amplified TXx increase in GCMs, COSMO_PHYS exhibits a stronger TXx increase compared to COSMO_NOPHYS in central and northern Europe, while in southern Europe the difference is only small (Figure 10). According to the difference between COSMO_PHYS and COSMO_NOPHYS, the contribution of plant physiological responses to the stronger TXx increase in GCMs compared to RCMs is around 81% in northern and 73% in central Europe (contribution to the median increase of all paired 21 GCM-RCM combinations). Note that the TXx signal in COSMO-CLM$_2$ is on the lower side compared to the RCM ensemble. We anticipate that this is not connected to the CLM land surface scheme, but more likely due to the fact that the driving GCM (MPI-ESM-LR) used to force COSMO-CLM2 shows a lower temperature change signal than many of the other GCMs in the EURO-CORDEX ensemble (Kjellström et al., 2018; Sørland et al., 2018).

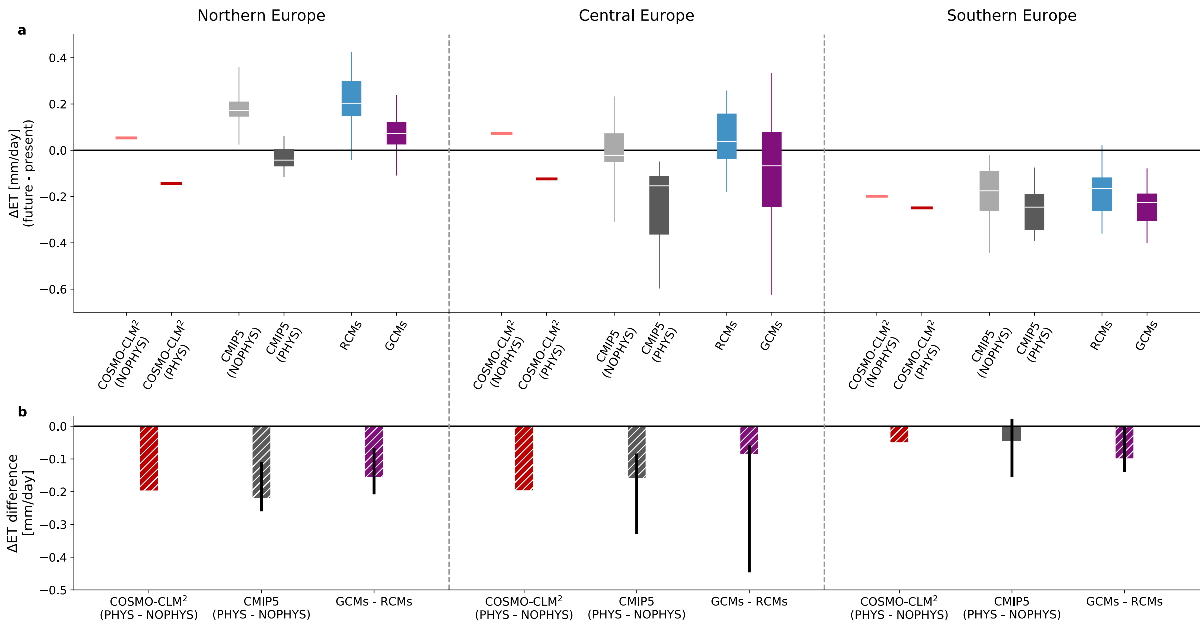

Figure 11: Change in summer evapotranspiration (ET) due to climate change and plant physiological CO_2 effects in three European regions. (a) Mean evapotranspiration changes (ΔET) between 1981–2010 and 2070–2099 for COSMO_NOPHYS (light red), COSMO_PHYS (red), RCMs (blue, number of models N=21), and GCMs (violet, N=9) and at 2070–2099 CO_2 concentrations relative to 1981–2010 CO_2 concentrations for CMIP5_NOPHYS (light grey, N=8) and CMIP5_PHYS (dark grey, N=8). The box-and-whisker-plots indicate the median (line), interquartile range (boxes), and total range (whiskers) of the ΔET distribution across climate models. (b) Difference of evapotranspiration changes (ΔET difference) between the PHYS and NOPHYS simulations of COSMO-CLM2 and the CMIP5 models (median difference, N=8) as well as the median difference of ΔET between the GCMs and RCMs (considering each RCM and subtracting its ΔET from the ΔET in the respective driving GCM, N=21). Black whiskers indicate the interquartile range and hatching denotes significant differences at the 5% level (calculated over 30 years for COSMO-CLM2 and over the different models for the CMIP5 models and the GCM-RCM difference; see Schwingshackl et al. 2018 for details).

The amplified TXx increase in COSMO_PHYS compared to COSMO_NOPHYS can be attributed to the stomatal response to elevated CO_2 concentrations in COSMO_PHYS. Smaller stomata openings lead to reduced evapotranspiration (ET), which affects atmospheric temperatures in two ways. Reduced evapotranspiration induces an increase of the fraction of net radiation that is converted to sensible heat flux, causing a stronger heating of near-surface air and affecting, in particular, extreme temperatures (Miralles et al., 2014; Perkins, 2015). Moreover, reduced evapotranspiration can induce cloud cover reductions, which leads to higher temperatures through enhanced incoming shortwave radiation. Indeed, future evapotranspiration in COSMO_PHYS is significantly reduced compared to COSMO_NOPHYS (Figure 11). Especially in central and northern Europe the evapotranspiration reduction is substantial (-0.20 mm/day), while in southern Europe it is only small (-0.05 mm/day).

Consistent with plant physiological responses, the nine driving GCMs of the 21 GCM-RCM model chains generally project a reduced evapotranspiration change compared to RCMs at the end of the 21st century (Figure 11). The difference between GCMs and RCMs is largest in northern Europe, where also COSMO-CLM2 and the CMIP5 models show strong evapotranspiration reductions due to plant physiological effects, and relatively small in southern Europe. Both the evapotranspiration reductions caused by plant physiological CO_2 responses and the evapotranspiration difference between RCMs and GCMs reveal a north-south gradient with strong evapotranspiration reductions in northern and small decreases in southern Europe, suggesting that a large part of the evapotranspiration difference between GCMs and RCMs can be explained by plant physiological responses. The respective evapotranspiration reductions are also consistent with the amplified TXx increase in GCMs compared to RCMs in northern and central Europe (Figure 10), indicating that a considerable percentage of the TXx difference between GCMs and RCMs is indeed due to plant physiological CO_2 responses.

7 Effects of irrigation and land-use changes on water cycle and resources

Using dedicated COSMO-CLM2 simulations (experiment (3) compared to experiment (1) as listed above), the project assessed how irrigation of agricultural crops affects projected changes of the hydrological cycle (as represented by the applied drought and water balance indices), as well as how simulated irrigation demands change from present to future climate conditions. The irrigation amount in COSMO-CLM2 is simulated dynamically for the fraction of the crop area being irrigated as prescribed from the present-day distribution of area equipped for irrigation (Section 2.1).

The climate-related irrigation demand reveals high amounts in Southern Europe and moderate amounts in Central Europe and Switzerland. Among the Swiss regions especially CHS shows substantial irrigation amounts. For Switzerland and CHS, the irrigation demand is projected to double until the end of the century.

Under both present and future climate conditions, irrigation is mostly limited to Southern and Central Europe (Figure 12, see also Figure A29 for a zoom on the Alpine area). Areas with substantial irrigation amounts are the Iberian Peninsula, Italy, the regions around the Black Sea and the Aegean, and the surroundings of the Nile. Future projections of irrigation amounts show that the regions where irrigation is important do not shift much, but within these regions and in surrounding areas the irrigation intensity strongly increases (Figure 12c). Moreover, it is worth noticing that there are no regions, where irrigation is projected to decrease.

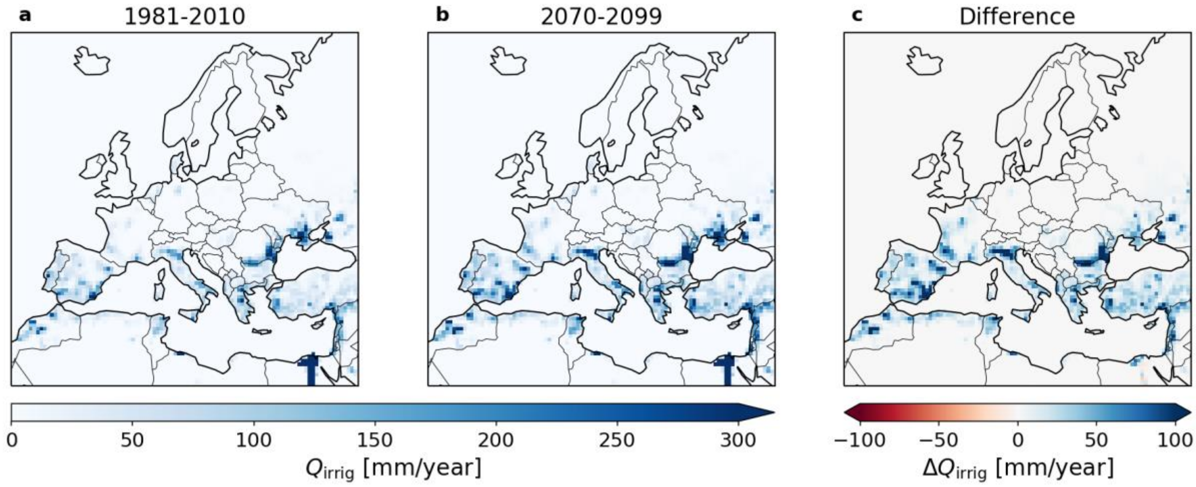

Figure 12: Yearly irrigation amount in COSMO-CLM2 during (a) 1981–2010 and (b) 2070–2099 and (c) the irrigation difference between the two time periods.

Figure 13 shows the average irrigation amounts per year in the different regions considered in this report, both for present and 2070–2099 climate conditions. The climate-related irrigation demand reveals high amounts in Southern Europe and moderate amounts in Central Europe and Switzerland. Among the Swiss regions especially CHS shows substantial irrigation amounts (see also Figure A29). For Switzerland and CHS, the irrigation demand is projected to double until the end of the century. Note that the high values in CHS might partly be caused by grid cells of the Po Valley included in this region, where irrigation is particularly high (Figure 12 and A29). All the other Swiss regions only exhibit negligible irrigation amounts.

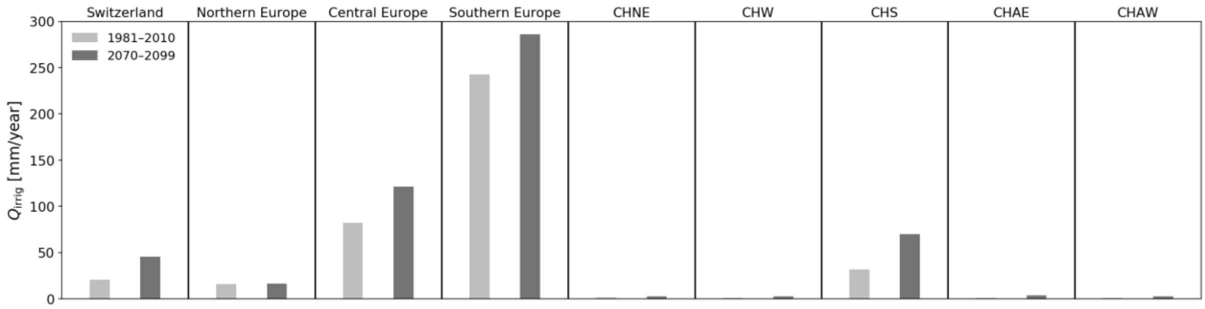

Figure 13: Yearly irrigation amount in COSMO-CLM$_2$ in the nine investigated regions during 1981–2010 and 2070–2099 (values representative for irrigated crop areas).

Including irrigation effects in COSMO-CLM$_2$ only leads to minor impacts on the future changes of the considered drought and water balance indices (see Section 5). Significant changes are only evident in Southern Europe, where *P-E* and *SRA* significantly decrease in the latest scenario period. The reduction of *SRA* is probably connected to the fact that the water for irrigation in COSMO-CLM$_2$ is taken from the runoff component, automatically reducing *SRA*. Besides these significant decreases, including irrigation leads to slight (but not significant) reductions in *CDD* and *SRA* and slight increases in *E*. In the Swiss regions CHS and CHAW irrigation further leads to a (non-significant) reduction in *SPI3* (Figure A23). The effect of irrigation on the investigated drought and water balance indices is overall only minor compared to climate change effects and, especially in Switzerland, the hydrological cycle is not much affected.

Land use change is potentially an additional important local driver of hydrological change in addition to climate. Simulations with two different versions of the CLM land surface model indicate however large uncertainties in the evapotranspiration response to land cover conversions at different altitude levels in Switzerland. This thus strongly limits our current predictive capacity to anticipate the hydrological outcome of land cover change in the Alpine context. Progress has been made in understanding and improving evapotranspiration's sensitivity to land cover change at the global scale thanks to the use of new observations (Meier et al., 2018), but understanding these processes in the Alpine context under strong elevation gradients and an associated lack of observational data still remains a research gap.

8 References

Alemohammad, S. H., Fang, B., Konings, A. G., Aires, F., Green, J. K., Kolassa, J., Miralles, D., Prigent, C. and Gentine, P.: Water, Energy, and Carbon with Artificial Neural Networks (WECANN): a statistically based estimate of global surface turbulent fluxes and gross primary productivity using solar-induced fluorescence, Biogeosciences, 14(18), 4101–4124, doi:10.5194/bg-14-4101-2017, 2017.

Alexander, L. V., Zhang, X., Peterson, T. C., Caesar, J., Gleason, B., Klein Tank, A. M. G., Haylock, M., Collins, D., Trewin, B., Rahimzadeh, F., Tagipour, A., Rupa Kumar, K., Revadekar, J., Griffiths, G., Vincent, L., Stephenson, D. B., Burn, J., Aguilar, E., Brunet, M., Taylor, M., New, M., Zhai, P., Rusticucci, M. and Vazquez-Aguirre, J. L.: Global observed changes in daily climate extremes of temperature and precipitation, J. Geophys. Res. Atmospheres, 111(D5), D05109, doi:10.1029/2005JD006290, 2006.

Byrne, M. P. and O'Gorman, P. A.: The Response of Precipitation Minus Evapotranspiration to Climate Warming: Why the "Wet-Get-Wetter, Dry-Get-Drier" Scaling Does Not Hold over Land, J. Clim., 28(20), 8078–8092, doi:10.1175/JCLI-D-15-0369.1, 2015.

CH2018: CH2018 – Climate Scenarios for Switzerland, National Centre for Climate Services., 2018.

Christensen, J. H. and Christensen, O. B.: A summary of the PRUDENCE model projections of changes in European climate by the end of this century, Clim. Change, 81(1), 7–30, doi:10.1007/s10584-006-9210-7, 2007.

Davin, E. L. and Seneviratne, S. I.: Role of land surface processes and diffuse/direct radiation partitioning in simulating the European climate, Biogeosciences, 9(5), 1695–1707, doi:10.5194/bg-9-1695-2012, 2012.

Davin, E. L., Stöckli, R., Jaeger, E. B., Levis, S. and Seneviratne, S. I.: COSMO-CLM$_2$: a new version of the COSMO-CLM model coupled to the Community Land Model, Clim. Dyn., 37(9), 1889–1907, doi:10.1007/s00382-011-1019-z, 2011.

Davin, E. L., Maisonnave, E. and Seneviratne, S. I.: Is land surface processes representation a possible weak link in current Regional Climate Models?, Environ. Res. Lett., 11(7), 074027, doi:10.1088/1748-9326/11/7/074027, 2016.

Dorigo, W., Wagner, W., Albergel, C., Albrecht, F., Balsamo, G., Brocca, L., Chung, D., Ertl, M., Forkel, M., Gruber, A., Haas, E., Hamer, P. D., Hirschi, M., Ikonen, J., Jeu, R. de, Kidd, R., Lahoz, W., Liu, Y. Y., Miralles, D., Mistelbauer, T., Nicolai-Shaw, N., Parinussa, R., Pratola, C., Reimer, C., Schalie, R. van der, Seneviratne, S. I., Smolander, T. and Lecomte, P.: ESA CCI Soil Moisture for improved Earth system understanding: State-of-the art and future directions, Remote Sens. Environ., doi:10.1016/j.rse.2017.07.001, 2017.

Frich, P., Alexander, L. V., Della-Marta, P., Gleason, B., Haylock, M., Tank, A. M. G. K. and Peterson, T.: Observed coherent changes in climatic extremes during the second half of the twentieth century, Clim. Res., 19(3), 193–212, 2002.

Greve, P. and Seneviratne, S. I.: Assessment of future changes in water availability and aridity, Geophys. Res. Lett., 42(13), 5493–5499, doi:10.1002/2015GL064127, 2015.

Gudmundsson, L. and Seneviratne, S. I.: Towards observation-based gridded runoff estimates for Europe, Hydrol Earth Syst Sci, 19(6), 2859–2879, doi:10.5194/hess-19-2859-2015, 2015.

Gudmundsson, L. and Seneviratne, S. I.: Observation-based gridded runoff estimates for Europe (E-RUN version 1.1), Earth Syst. Sci. Data, 8(2), 279–295, doi:10.5194/essd-8-279-2016, 2016.

Haylock, M. R., Hofstra, N., Tank, A. M. G. K., Klok, E. J., Jones, P. D. and New, M.: A European daily high-resolution gridded data set of surface temperature and precipitation for 1950–2006, J. Geophys. Res. Atmospheres, 113(D20), doi:10.1029/2008JD010201, 2008.

Hong, T., Dong, W., Ji, D., Dai, T., Yang, S. and Wei, T.: The response of vegetation to rising CO_2 concentrations plays an important role in future changes in the hydrological cycle, Theor. Appl. Climatol., doi:10.1007/s00704-018-2476-7, 2018.

Isotta, F. A., Frei, C., Weilguni, V., Tadić, M. P., Lassègues, P., Rudolf, B., Pavan, V., Cacciamani, C., Antolini, G., Ratto, S. M., Munari, M., Micheletti, S., Bonati, V., Lussana, C., Ronchi, C., Panettieri, E., Marigo, G. and Vertačnik, G.: The climate of daily precipitation in the Alps: development and analysis of a high-resolution grid dataset from pan-Alpine rain-gauge data, Int. J. Climatol., 34(5), 1657–1675, doi:10.1002/joc.3794, 2014.

Jacob, D., Petersen, J., Eggert, B., Alias, A., Christensen, O. B., Bouwer, L. M., Braun, A., Colette, A., Déqué, M., Georgievski, G., Georgopoulou, E., Gobiet, A., Menut, L., Nikulin, G., Haensler, A., Hempelmann, N., Jones, C., Keuler, K., Kovats, S., Kröner, N., Kotlarski, S., Kriegsmann, A., Martin, E., van Meijgaard, E., Moseley, C., Pfeifer, S., Preuschmann, S., Radermacher, C., Radtke, K., Rechid, D., Rounsevell, M., Samuelsson, P., Somot, S., Soussana, J.-F., Teichmann, C., Valentini, R., Vautard, R., Weber, B. and Yiou, P.: EURO-CORDEX: new high-resolution climate change projections for European impact research, Reg. Environ. Change, 14(2), 563–578, doi:10.1007/s10113-013-0499-2, 2014.

Jung, M., Reichstein, M. and Bondeau, A.: Towards global empirical upscaling of FLUXNET eddy covariance observations: validation of a model tree ensemble approach using a biosphere model, Biogeosciences, 6(10), 2001–2013, doi:10.5194/bg-6-2001-2009, 2009.

Kjellström, E., Nikulin, G., Strandberg, G., Christensen, O. B., Jacob, D., Keuler, K., Lenderink, G., Meijgaard, E. van, Schär, C., Somot, S., Sørland, S. L., Teichmann, C. and Vautard, R.: European climate change at global mean temperature increases of 1.5 and 2 °C above pre-industrial conditions as simulated by the EURO-CORDEX regional climate models, Earth Syst. Dyn., 9(2), 459–478, doi:10.5194/esd-9-459-2018, 2018.

Lemordant, L. and Gentine, P.: Vegetation Response to Rising CO_2 Impacts Extreme Temperatures, Geophys. Res. Lett., 46(3), 1383–1392, doi:10.1029/2018GL080238, 2019.

Lemordant, L., Gentine, P., Swann, A. S., Cook, B. I. and Scheff, J.: Critical impact of vegetation physiology on the continental hydrologic cycle in response to increasing CO_2, Proc. Natl. Acad. Sci., 115(16), 4093–4098, doi:10.1073/pnas.1720712115, 2018.

Lloyd-Hughes, B. and Saunders, M. A.: A drought climatology for Europe, Int J. Climatol., 22(13), 1571–1592, 2002.

Martens, B., Miralles, D. G., Lievens, H., Schalie, R. van der, Jeu, R. A. M. de, Fernández-Prieto, D., Beck, H. E., Dorigo, W. A. and Verhoest, N. E. C.: GLEAM v3: satellite-based land evaporation and root-zone soil moisture, Geosci. Model Dev., 10(5), 1903–1925, doi:10.5194/gmd-10-1903-2017, 2017.

McKee, T. B., Doesken, N. J. and Kleist, J.: The relationship of drought frequency and duration to time scales, Eighth Conference on Applied Climatology, Anaheim, California, USA., 1993.

Meier, R., Davin, E. L., Lejeune, Q., Hauser, M., Li, Y., Martens, B., Schultz, N. M., Sterling, S. and Thiery, W.: Evaluating and improving the Community Land Model's sensitivity to land cover, Biogeosciences, 15(15), 4731–4757, doi:10.5194/bg-15-4731-2018, 2018.

Miralles, D. G., Teuling, A. J., van Heerwaarden, C. C. and Vila-Guerau de Arellano, J.: Mega-heatwave temperatures due to combined soil desiccation and atmospheric heat accumulation, Nat. Geosci., 7, 345–349, doi:10.1038/ngeo2141, 2014.

Mueller, B., Hirschi, M., Jimenez, C., Ciais, P., Dirmeyer, P. A., Dolman, A. J., Fisher, J. B., Jung, M., Ludwig, F., Maignan, F., Miralles, D. G., McCabe, M. F., Reichstein, M., Sheffield, J., Wang, K., Wood, E. F., Zhang, Y. and Seneviratne, S. I.: Benchmark products for land evapotranspiration: LandFlux-EVAL multi-data set synthesis, Hydrol. Earth Syst. Sci., 17(10), 3707–3720, doi:10.5194/hess-17-3707-2013, 2013.

Oleson, K. W., Lawrence, D. M., B, G., Flanner, M. G., Kluzek, E., J, P., Levis, S., Swenson, S. C., Thornton, E., Feddema, J., Heald, C. L., Jean-francois Lamarque, Niu, G., Qian, T., Running, S., Koichi Sakaguchi, Yang, L., Zeng, X., Zeng, X. and Mark Decker: Technical Description of version 4.0 of the Community Land Model (CLM), NCAR., 2010.

Orlowsky, B. and Seneviratne, S. I.: Elusive drought: uncertainty in observed trends and short- and long-term CMIP5 projections, Hydrol. Earth Syst. Sci., 17(5), 1765–1781, doi:10.5194/hess-17-1765-2013, 2013.

Orth, R. and Seneviratne, S. I.: Introduction of a simple-model-based land surface dataset for Europe, Environ. Res. Lett., 10(4), doi:10.1088/1748-9326/10/4/044012, 2015.

Perkins, S. E.: A review on the scientific understanding of heatwaves—Their measurement, driving mechanisms, and changes at the global scale, Atmospheric Res., 164–165, 242–267, doi:10.1016/j.atmosres.2015.05.014, 2015.

Riahi, K., Rao, S., Krey, V., Cho, C., Chirkov, V., Fischer, G., Kindermann, G., Nakicenovic, N. and Rafaj, P.: RCP 8.5–A scenario of comparatively high greenhouse gas emissions, Clim. Change, 109(1–2), 33–57, doi:10.1007/s10584-011-0149-y, 2011.

Schwingshackl, C., Davin, E. L., Hirschi, M., Sørland, S. L., Wartenburger, R. and Seneviratne, S. I.: Regional climate model projections underestimate future warming due to missing plant physiological CO_2 response, Environ. Res. Lett., 14(11), doi:10.1088/1748-9326/ab4949, 2019.

Seneviratne, S. I., Nicholls, N., Easterling, D., Goodess, C. M., Kanae, S., Kossin, J., Luo, Y., Marengo, J., McInnes, K., Rahimi, M., Reichstein, M., Sorteberg, A., Vera, C. and Zhang, X.: Changes in climate extremes and their impacts on the natural physical environment, in Managing the Risks of Extreme Events and Disasters to Advance Climate Change Adaptation, edited by C. B. Field, V. Barros, T. F. Stocker, D. Qin, D. J. Dokken, K. L. Ebi, M. D. Mastrandrea, K. J. Mach, G.-K. Plattner, S. K. Allen, M. Tignor, and P. M. Midgley, pp. 109–230, Cambridge University Press, Cambridge, United Kingdom and New York, NY, USA. [online] Available from: http://ipcc-wg2.gov/SREX/, 2012.

Seneviratne, S. I., Donat, M. G., Pitman, A. J., Knutti, R. and Wilby, R. L.: Allowable CO_2 emissions based on regional and impact-related climate targets, Nature, 529, 477–483, doi:10.1038/nature16542, 2016.

Skinner, C. B., Poulsen, C. J. and Mankin, J. S.: Amplification of heat extremes by plant CO_2 physiological forcing, Nat. Commun., 9(1), 1094, doi:10.1038/s41467-018-03472-w, 2018.

Sørland, S. L., Schär, C., Lüthi, D. and Kjellström, E.: Bias patterns and climate change signals in GCM-RCM model chains, Environ. Res. Lett., 13(7), 074017, doi:10.1088/1748-9326/aacc77, 2018.

Swann, A. L. S., Hoffman, F. M., Koven, C. D. and Randerson, J. T.: Plant responses to increasing CO_2 reduce estimates of climate impacts on drought severity, Proc. Natl. Acad. Sci., 113(36), 10019–10024, doi:10.1073/pnas.1604581113, 2016.

Tebaldi, C., Hayhoe, K., Arblaster, J. M. and Meehl, G. A.: Going to the Extremes, Clim. Change, 79(3–4), 185–211, doi:10.1007/s10584-006-9051-4, 2006.

Wartenburger, R., Hirschi, M., Donat, M. G., Greve, P., Pitman, A. J. and Seneviratne, S. I.: Changes in regional climate extremes as a function of global mean temperature: an interactive plotting framework, Geosci. Model Dev., 10(9), 3609–3634, doi:10.5194/gmd-10-3609-2017, 2017.